AIMS Materials Science, 12(4): 744–754.
DOI: 10.3934/matersci.2025032
Received: 20 May 2025
Revised: 19 July 2025
Accepted: 30 July 2025
Published: 05 August 2025

http://www.aimspress.com/journal/Materials

Research article

Observation of memory effects in 5CB/PVAc liquid crystal-polymer composites

Timur A. Chimytov[1,2], Andrey V. Nomoev[1,2], Sergey V. Kalashnikov[2], Michael I. Ojovan[3,4,*], Migmar V. Darmaev[1,2], Alexey A. Mashanov[1] and Tuyana B. Kim[1]

[1] Banzarov Buryat State University, Ulan-Ude, 670000, Russia
[2] Institute of Physical Materials Science, Siberian Branch of the Russian Academy of Sciences, Ulan-Ude, 670047, Russia
[3] School of Chemical, Materials and Biological Engineering, The University of Sheffield, Sheffield S1 3JD, United Kingdom
[4] Department of Radiochemistry, Lomonosov Moscow State University, Moscow, 119991, Russia

* **Correspondence:** Email: m.ojovan@sheffield.ac.uk; Tel: +44-788-389-1379.

Abstract: A study of the memory effect in polymer-dispersed liquid crystal composites based on 4-cyano-4'-pentylbiphenyl (5CB) and polyvinyl acetate (PVAc) obtained by solvent-induced phase separation is presented. Using an original high-precision bridge circuit, it is demonstrated that a cyclic voltage application causes conditionally irreversible capacitance changes exclusively in 5CB/PVAc = 2/1 composites, with the memory parameter $M = 0.17$ after the first polarization cycle. The effect shows a limited accumulation (M increases only to 0.19 in subsequent cycles) and can be completely eliminated by heating above the temperature of the nematic-isotropic transition. Polarization microscopy revealed key morphological differences: the liquid crystal is displaced into homogeneous spherical droplets (50–70 μm) in the 5CB/PVAc = 1/1 composites, while the 2/1 systems exhibit complex phase delamination with characteristic "four-leaf clover" defects (50–200 μm) containing disclinations with a winding number of +1. This morphology indicates the tangential orientation of 5CB at the polymer interfaces. The short-term thermal effect destroys these clover structures, thus forming 10 μm domains and eliminating the director field configuration required for memory retention. The memory effect originates from metastable director configurations in non-spherical cavities, where surface anchoring enables degenerate axes aligned with the applied field. The demonstrated effects enable novel functional devices based on electrically programmable LC-polymer memory systems.

Keywords: smart glasses; liquid crystals; PVAc; polymer composites; PDLC; memory effect

1. Introduction

Liquid crystal (LC) systems continue to drive innovation in smart materials, thereby combining tunable optical properties with versatile functionality. Recent advances in soft-matter photonics have demonstrated remarkable progress in light manipulation using LC-based materials [1], while stimuli-responsive liquid crystal polymers highlight new possibilities for adaptive systems [2]. These developments create a strong technological foundation for practical applications of liquid crystal composites. Polymer dispersed liquid crystals (PDLCs) have a number of key advantages that make them in demand for various applications, including smart glasses, displays, and adaptive optics [3]. PDLC-based smart glasses consist of thin films in which LC droplets are dispersed in a polymer matrix [4]. In the absence of a field, the LC molecules are randomly oriented, which is why the light is strongly scattered at the LC/polymer interface, making the glass matte. When a voltage is applied, the LC molecules orient themselves along the field, and if the refractive indices of the LC and the polymer are equal, then the glass becomes transparent. Among the main advantages of PDLC glass over other technologies are mechanical stability and resistance to long-term external influences. Additionally, such devices have sufficient energy efficiency, since a current is only required during switching, and energy is not consumed in stable states. In addition to mechanical and electro-optical properties, some types of PDLC glasses are distinguished by the electromechanical memory effect: after a sequential application and the removal of the electric field, the transparency of such glasses does not return to its original state. This makes it possible to create non-volatile optical devices.

Early studies on the electro-optical properties of ultraviolet (UV)-cured PDLCs revealed that a strong memory effect occurs in systems where the morphology consists of numerous interconnected LC-filled cavities rather than isolated LC microdroplets [5,6]. This memory can be erased by PDLC heating, which temporarily destroys the nematic order in the LC. The dependence of the memory effect on morphology was also shown in [7], which studied PDLCs made using the polymerization-induced phase separation (PIPS) method, where a strong memory effect was found in those PDLCs in which the polymer matrix was a complex structure of relatively isolated micron-sized polymer beads. Additionally, the memory effect was found in liquid crystal suspensions doped with various nanoparticles: ferroelectric [8,9], magnetic, and non-magnetic nanoparticles [10,11].

One possible explanation for the memory effect in PDLCs could involve the formation of stable topological defects (disclinations) in the liquid crystal phase, where the orientational order of molecules is disrupted near these defects [12]. Such defects are able to stabilize the metastable configurations of the director, thus preventing the complete restoration of the initial state after the removal of the electric field. Their formation may be associated with phase transitions during heating-cooling or with a disruption of the anchoring conditions at the polymer matrix surface [13]. It is noteworthy that disclinations themselves can act as centers of local disordering [14], thus contributing to the consolidation of inhomogeneities in the orientation of the LC. However, the impact of topological defects on the electro-optical properties of PDLCs, including the memory effect, remains poorly understood, thus underscoring the relevance of further research in this area. Understanding the role of disclination could open up new ways to manage state memory in PDLC systems to create energy-efficient switchable devices.

This paper presents the results of an experimental study of the dielectric and morphological properties of PDLC composites based on nematic LC 4-Cyano-4'-pentylbiphenyl (5CB) and polyvinyl acetate polymer (PVAc) and the identification of the memory effect.

2. Materials and methods

PVAc, 5CB, and the organic solvents benzene and acetone were used as materials to manufacture the PDLC film. The choice of PVAc and 5CB as the main materials for the PDLC is based on previous studies of these films [15]. Note that the refractive index of PVAc is close to the normal refractive index for 5CB (1.47 and 1.53, respectively), thus ensuring sufficient transparency of the samples in the switched-on state (when the field is applied). The phase transition temperatures for the 5CB crystal-nematic and nematic-isotropic are T_{CN} = 22.5 °C and T_{NI} = 35 °C, respectively.

Samples with the PDLC films were made using the Solvent-Induced Phase Separation (SIPS) method, based on the phase separation of LC and polymer during the evaporation of solvents. The PDLC preparation process consisted of the following steps. The PVAc solution (10%) was mechanically mixed with 5CB, and then the resulting mixture was ultrasonicated (28 kHz, 100 W) for 10 min to effectively disperse the LC in the polymer. After treatment, the emulsion was deposited onto indium tin oxide (ITO)-coated glass using spin-coating (3000 rpm, 20 sec). After air-drying at 25 °C for 30 min, the emulsion was coated with a second glass and the samples were subjected to thermal shock (heating in a furnace at 125 °C for 5 min). The thickness of the films in the resulting samples was 19–21 μm. In this way, two batches of PDLC samples with different 5CB content were produced: 5CB/PVAc = 1/1 and 5CB/PVAc = 2/1, by weight. To study the morphology of the films, an LOMO MIKMED-6 polarization microscope (POM) and a JEOL Neoscope II JCM-6000 scanning electron microscope (SEM) were used. The following are the results of the study for representative samples from these batches.

To measure the dielectric anisotropy in samples of LC cells, a measuring device that contained an alternating current bridge was created [16]. This setup differs from conventional bridges in that a constant bias voltage of up to 120 V can be applied to the sample directly when measuring the electrical capacitance, which changes the orientation of the liquid crystals in the sample [17]. At the same time, the field strength in the sample reached up to 6 V/μm. The bridge operated at a fixed frequency of 10 kHz during measurements (adjustable range: 1–30 kHz). This frequency was selected to ensure a minimal molecular response of the liquid crystals to the probing electric field. The capacitance error in the range of 100–700 pF is below 5%. In addition to the capacitance, the dielectric loss tangent can be measured, which served as a quality control parameter for the fabricated samples.

3. Results and discussion

Figure 1 presents the capacitance measurements of both samples as a function of the applied electric field. The arrows indicate the directions of the field change during measurements. As expected, the higher 5CB content sample exhibits both a greater average capacitance and a wider variation range. This behavior can be attributed to the increased LC free volume in the 5CB/PVAc = 2/1 sample, thereby reducing the influence of interfacial anchoring forces at the LC-PVAc boundary. In fact, the reorientation of the 5CB molecules in the 5CB/PVAc = 2/1 sample initiates at lower electric field strengths compared to the 1/1 composition. The threshold electric field that corresponds to 10% of the

maximum capacitance value for the 5CB/PVAc = 2/1 sample is 0.3 V/μm, while this value rises to 1 V/μm for the 5CB/PVAc = 1/1 sample.

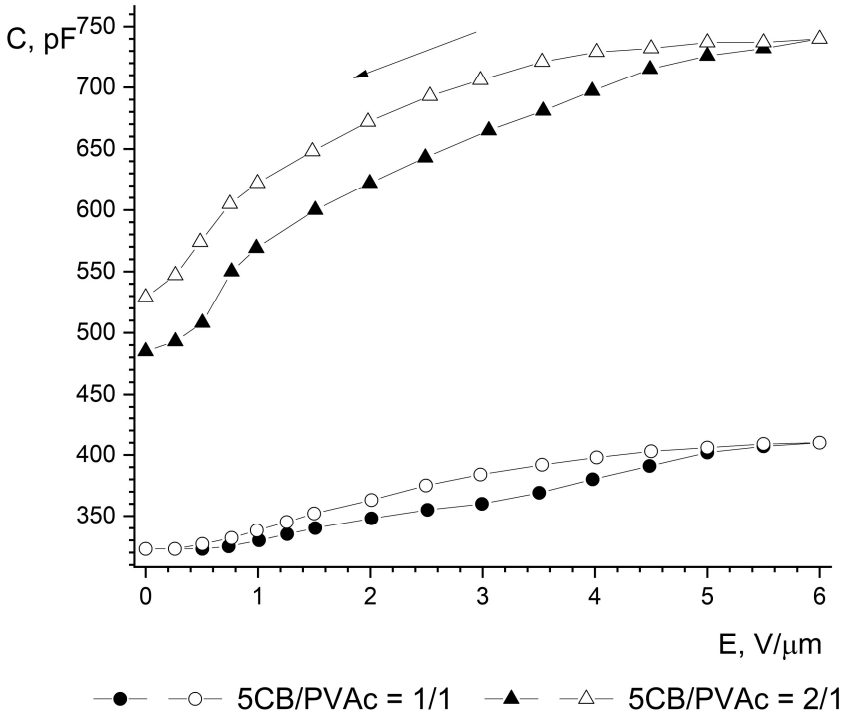

Figure 1. Capacitance versus the bias electric field.

In addition, the change in capacitance of both samples demonstrates hysteresis. However, unlike a sample with a lower 5CB content, the capacity of a sample with 5CB/PVAc = 2/1 does not return to its original value after the field is removed.

For clarity, Figure 2 presents the normalized capacitance change using the following formula: $\Delta C/C_0 = (C_E - C_0)/C_0$, where C_E and C_0 are the field-dependent and initial capacitance (at $E = 0$), respectively. The 5CB/PVAc = 2/1 sample shows approximately 9% persistent capacitance increase after polarization cycling, thus demonstrating a clear electromechanical memory behavior. To quantify this effect, we introduce the memory parameter M as follows (Eq 1):

$$M = \frac{C_{off} - C_0}{C_{on} - C_0} \tag{1}$$

where C_0, C_{on}, and C_{off} are the initial capacity of the sample, the capacity at the maximum field, and the residual capacity after field removal, respectively. Thus, $M = 0.17$ for the 5CB/PVAc = 2/1 sample, and $M = 0$ for the 5CB/PVAc = 1/1 sample.

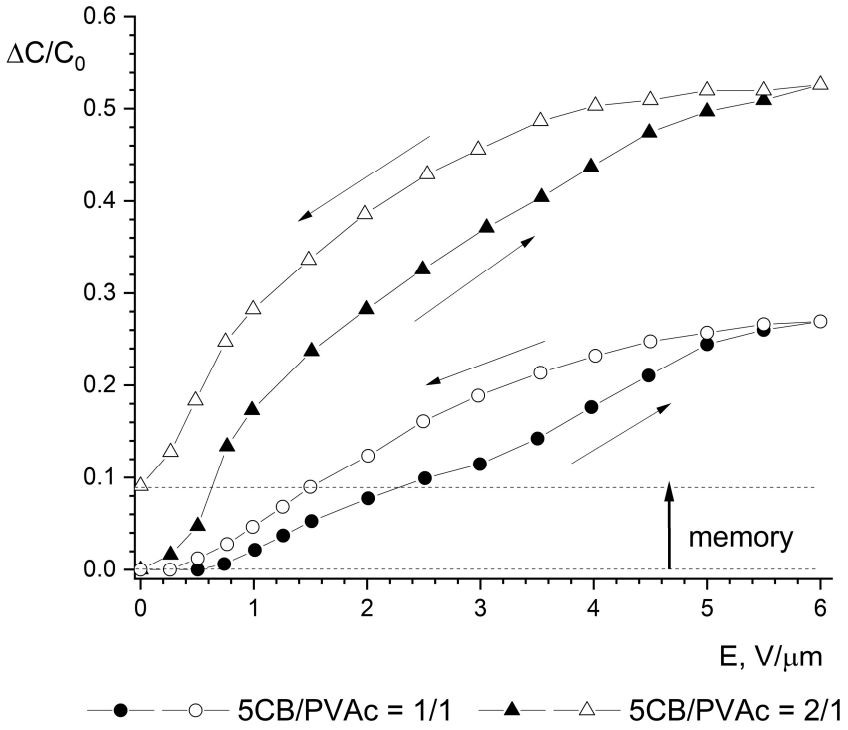

Figure 2. Normalized capacitance versus the bias electric field.

To determine the memory accumulation effect on the 5CB/PVAc = 2/1 samples, additional measurements were performed: the sample was subjected to an additional cycle of polarization by an electric field. Figure 3 shows the results of capacitance-voltage measurements: the right-hand region ($E > 0$) corresponds to the first polarization cycle, while the left-hand region ($E < 0$) represents the second cycle. The graph shows that the amount of memory growth after an additional field application is relatively small: the memory parameter after the first cycle ($M = 0.17$) grows to $M = 0.19$. Notably, the sample's maximum capacitance values remain consistent across both polarization cycles, with $\Delta C/C_0 = 0.53$ in each case. The very observation of memory accumulation after the second polarization cycle indicates the existence of multiple metastable LC states. These states are sufficiently close in energy, which allows the system to spontaneously relax from one metastable state to another over time. The experimental data suggest that this relaxation typically occurs on the timescale of several minutes. Consequently, the memory accumulation effect induced by additional polarization cycles is highly limited and short-lived.

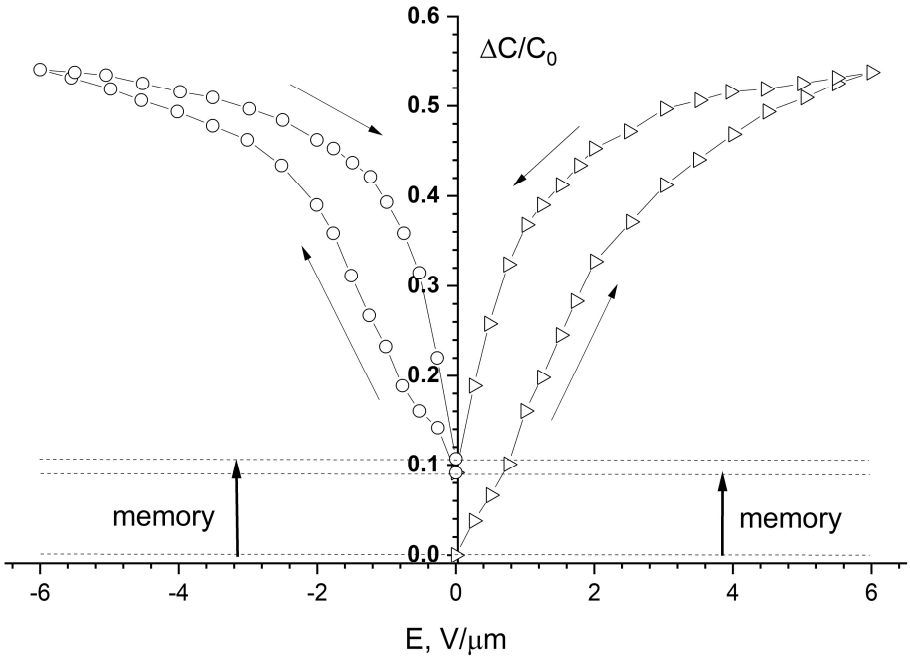

Figure 3. Normalized capacitance versus the bias electric field: two polarization cycles.

Figures 4 and 5 show micrographs of samples obtained using the POM. The 5CB/PVAc = 1/1 sample (Figure 4) exhibits a homogeneous morphology: most of the image shows a granular area that corresponds to a liquid crystal encapsulated in a PDLC polymer matrix. As seen in Figure 6, the PDLC exhibits a 'Swiss cheese' morphology, which is characterized by isolated droplets with sizes up to 10 μm. Additionally, as shown in Figure 4, 100–150 μm domains are observed, where the liquid crystal is displaced from the polymer volume (visible as dark rings), thus forming relatively large droplets (50–70 μm in size). The 5CB/PVAc = 2/1 sample (Figure 5a) is much less homogeneous: the dark caverns that correspond to the isotropic polymer without LC are comparable to the sizes of the granular PDLC domains. Droplets of displaced LCs in the image appear as large four-leaf clovers up to 200 μm, which are chaotically distributed over the surface of dark caverns.

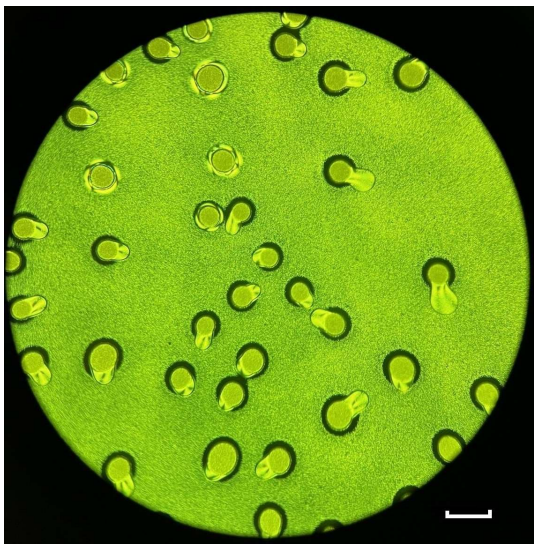

Figure 4. POM micrograph of the sample 5CB/PVAc = 1/1, scale: 150 μm.

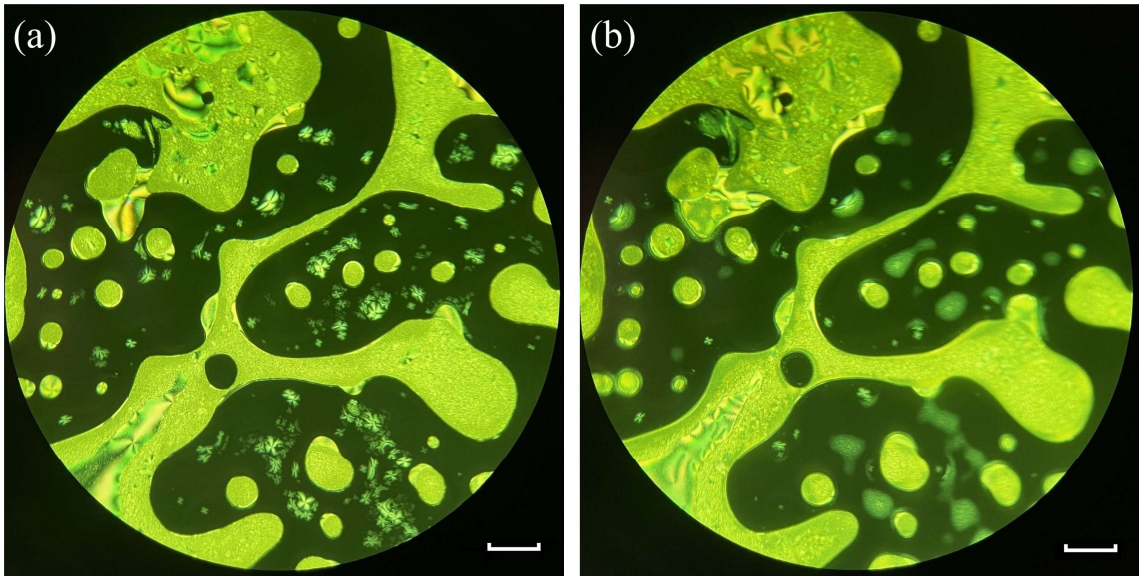

Figure 5. POM micrograph of the sample 5CB/PVAc = 2/1. (a) Before heating. (b) After heating. Scale: 150 μm.

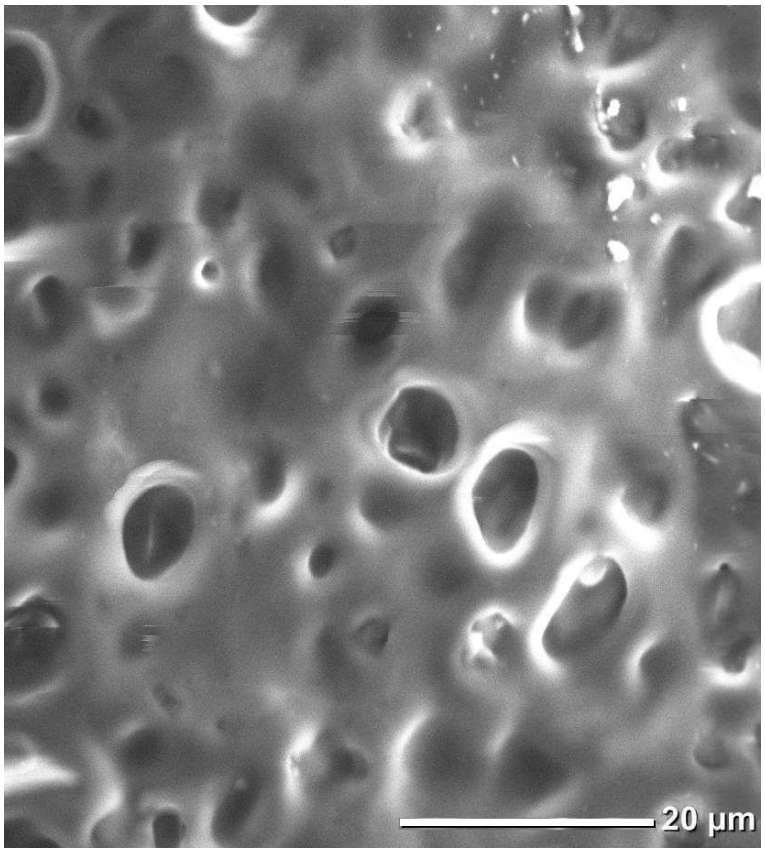

Figure 6. SEM micrograph of the PDLC film. Scale: 20 μm.

The appearance of four-leaf clover patterns in the POM images results from distortion in the director field inside the LC droplets. It is known that 5CB is characterized by a tangential orientation

of the LC molecules at the PVAc interface. This LC alignment should cause the director field inside the droplets to form bipolar patterns that converge toward topological defects (disclinations) at their polars. The winding number m, which characterizes the strength of disclinations, is determined from Eq 2:

$$2\pi m = \oint d\theta \tag{2}$$

where integration is performed over the argument θ (the tilt angle of the LC director relative to the fixed axis) along a closed loop around the disclination kernel. The winding number takes positive values if the director rotates in the same direction as the loop traversal (clockwise/counterclockwise). The number of dark stripes in cloverleaf patterns under crossed polarizers indicates how many times the LC director rotates by π/2 during a full circuit around the disclination core. Since all cloverleaf patterns in Figure 5a exhibit four dark brushes (which were confirmed to rotate in the same direction as the polarizers), the director consequently rotates 2π, thus yielding m = +1. This indirectly confirms the assumption of the tangential orientation of 5CB molecules in droplets displaced from the polymer.

As previously stated, one way to reset the memory involves heating the sample above T_{NI}. Figure 5b shows a POM micrograph of the 5CB/PVAc = 2/1 sample with an induced memory after short-term heating to 400 K. Here, the large four-leaf clover patterns have predominantly fragmented into smaller (~10 μm) anisotropic structures. Thus, the orientation of the 5 CB molecules inside the droplets displaced from the polymer changed. If we assumed a tangential orientation in the entire volume of individual droplets before heating the sample, then each droplet contains multiple subdomains with an independent LC orientation.

For 5CB/PVAc composites, the planar orientation of the 5CB molecules at the PVAc interface can be attributed to specific dipole-dipole interactions between the polar groups of the components, which results in the attraction of the LC cyanogroups to the polymer surface. The estimate of the interaction energy between the –C≡N and –$OCOCH_3$ polar groups for the 5CB and PVAc molecules, respectively, can be determined from Eq 3 [18]:

$$E_{dd} = -\frac{u_1 u_2}{4\pi\varepsilon\varepsilon_0 r^3} f(\theta) \tag{3}$$

where $u_{1,2}$ are the dipole moments of the –C≡N and –$OCOCH_3$ groups (3.6 D and 1.8 D, respectively), r is the characteristic intermolecular distance (approximately 0.5 nm), and $f(\theta)$ is the orientation factor, which has a maximum with the mutually parallel orientation of the molecules ($fmax = 2$). The estimate of the planar orientation gives $E_{dd} \approx -3 \times 10^{-21}$ J. The thermal energy transferred to the molecules when heated is equal to $E_T = k(T - T_{NI}) \approx 4 \times 10^{-21}$ J, which gives a comparable value with E_{dd}. The comparable magnitudes of these energies explain the heat-induced disruption of LC alignment within droplets, which—as evident in Figure 5b—remains irreversible upon subsequent cooling. In addition to the dipole-dipole interaction, it is necessary to take quantum effects, the presence of weak hydrogen bonds, and the presence of ionic impurities into account to fully describe the interaction of the LC with the polymer.

Distortion of the 5CB orientational order at the interface with the polymer matrix appears to play a key role in the mechanisms of memory effect formation in systems with liquid crystal droplets displaced from the polymer. As demonstrated in [7], the memory effect in LC composites arises from modified anchoring conditions at the polymer surface and the formation of additional degenerate directions (axes) near this surface, along which the LC molecules relax after the removal of the external

field. In 5CB/PVAc = 1/1 composites, the LC is preferentially displaced into droplets of an almost spherical shape (Figure 4), where degenerate metastable axes are not formed. In contrast, in systems with a ratio of 5CB/PVAc = 2/1, a complex pattern of defects-disclination is observed (Figure 5a,b), which indicates the formation of a non-trivial structure of the LC in the volume displaced from the polymer matrix. Under such conditions, the restrictions associated with the fixation of molecules in spherical droplets are probably weakened, which leads to the appearance of degenerate axes. It is noteworthy that the increased capacity of the composite in the memory state compared to the initial unperturbed state indicates the preferential orientation of these axes along the direction of the external field. A violation of the initial orientation of the LC (for example, during heating) causes a reorientation of degenerate axes and, as a result, memory erasure.

4. Conclusions

In this work, composite materials based on a nematic LC of 5CB and PVAc with varying mass ratios of components were synthesized using the SIPS method. The study of their electrophysical characteristics was performed using a custom measuring system developed by the authors.

It has been experimentally established that the application of an external electric field induces a hysteresis response in dielectric permittivity. It is noteworthy that a pronounced effect of the electrical state memory was only observed in composites with a ratio of 5CB/PVAc = 2/1, while additional field switching cycles did not lead to significant memory accumulation.

A morphological analysis by POM revealed significant structural differences between the composites. Samples with a ratio of 5CB/PVAc = 2/1 showed a high degree of heterogeneity and a complex defect topology, which was characterized by a predominance of four-leaf clover disclinations. Such morphology indicates the tangential orientation of the LC molecules in droplets displaced from the polymer matrix. It is important to note that the thermal treatment that results in a distortion of 5CB molecular orientation completely eliminates the memory effect.

The obtained results are of scientific and practical interest for the development of functional materials with controllable dielectric properties and reproducible memory effects. The most promising areas of further research include the systematic optimization of the composition of composites to enhance and stabilize the memory effect, as well as the creation of theoretical models that establish quantitative correlations between the morphological features of the structure and the electrophysical characteristics of the obtained materials.

Use of AI tools declaration

The authors declare they have not used Artificial Intelligence (AI) tools in the creation of this article.

Acknowledgments

This work was supported by the state assignment of the Institute of Physical Materials Science, Siberian Branch of the Russian Academy of Sciences (Project No. FWSF-2024-0013) “Development of physical principles for creating functional composite nanostructures and materials, and modeling of phase diagrams in multicomponent systems”.

Author contributions

Timur A. Chimytov: writing-original draft, analysis and interpretation of results; Andrey V. Nomoev: funding acquisition, supervision; Sergey V. Kalashnikov: experimental setup development; Michael I. Ojovan: writing-review, editing; Migmar V. Darmaev: editing, visualization; Alexey A. Mashanov: editing, data collection; Tuyana B. Kim: data collection.

Conflict of interest

Michael I. Ojovan is on a special issue editorial board for *AIMS Materials Science* and was not involved in the editorial review or the decision to publish this article. All authors declare that there are no competing interests.

References

1. Zhang Y, Zheng ZG, Li Q (2024) Multiple degrees-of-freedom programmable soft-matter-photonics: Configuration, manipulation, and advanced applications. *Responsive Mater* 2: e20230029. https://doi.org/10.1002/rpm.20230029
2. Lan R, Hu XG, Chen J, et al. (2024) Adaptive liquid crystal polymers based on dynamic bonds: From fundamentals to functionalities. *Responsive Mater* 2: e20230030. https://doi.org/10.1002/rpm.20230030
3. Ye Y, Guo L, Zhong T (2023) A review of developments in polymer stabilized liquid crystals. *Polymers* 15: 2962. https://doi.org/10.3390/polym15132962
4. Islam MS, Chan KY, Thien GSH, et al. (2023) Performances of polymer-dispersed liquid crystal films for smart glass applications. *Polymers* 15: 3420. https://doi.org/10.3390/polym15163420
5. Yamaguchi R, Sato S (1991) Memory effects of light transmission properties in polymer-dispersed-liquid-crystal (PDLC) films. *Jpn J Appl Phys* 30: L616–L616. https://doi.org/10.1143/JJAP.30.L616
6. Yamaguchi R, Sato S (1992) Highly transparent memory states by phase transition with a field in polymer dispersed liquid crystal films. *Jpn J Appl Phys* 31: L254–L256. https://doi.org/10.1143/JJAP.31.L254
7. Han J (2003) Memory and depolarization effects of polymer-dispersed liquid crystal films based on E7/NOA61. *J Korean Phys Soc* 43: 45–50. Available from: https://www.jkps.or.kr/journal/download_pdf.php?spage=45&volume=43&number=1.
8. Basu R (2014) Soft memory in a ferroelectric nanoparticle-doped liquid crystal. *Phys Rev E* 89: 022508. https://doi.org/10.1103/PhysRevE.89.022508
9. Kempaiah R, Liu Y, Nie Z, et al. (2016) Giant soft-memory in liquid crystal nanocomposites. *Appl Phys Lett* 108: 083105. http://dx.doi.org/10.1063/1.4942593
10. Gdovinová V, Tomašovičová V, Jeng SC, et al. (2019) Memory effect in nematic phase of liquid crystal doped with magnetic and non-magnetic nanoparticles. *J Mol Liq* 282: 286–291. https://doi.org/10.1016/j.molliq.2019.03.001
11. Bury P, Veveričík M, Černobila F, et al. (2023) Study on the memory effect in aerosil-filled nematic liquid crystal doped with magnetic nanoparticles. *Nanomaterials* 13: 2987. https://doi.org/10.3390/nano13232987

12. Fumeron S, Berche B (2023) Introduction to topological defects: From liquid crystals to particle physics. *Eur Phys J Spec Top* 232: 1813–1833. https://doi.org/10.1140/epjs/s11734-023-00803-x
13. Angelo J, Culbreath C, Yokoyama H (2017) Breaking planar liquid crystal anchoring to form controllable twist disclination loops. *Mol Cryst Liq Cryst* 646: 214–219. https://doi.org/10.1080/15421406.2017.1287486
14. Han A, Lagerwall J, Majumdar A (2024) Topological defects as nucleation points of the nematic-isotropic phase transition in liquid crystal shells. *Phys Rev E* 109: 064702. https://doi.org/10.1103/PhysRevE.109.064702
15. Zharkova GM, Fomichev VP, Podyacheva OYu (2019) Formation of polymer-dispersed nematic liquid crystals doped by nitrogen-containing carbon nanotubes in magnetic field. *Liq Cryst Appl* 19: 51–58. https://doi.org/10.18083/LCAppl.2019.3.51
16. Kalashnikov SV, Romanov NA, Nomoev AV (2021) Installation for measuring the dielectric anisotropy of liquid crystals at low frequencies by the bridge method with constant displacement. *IOP Conf Ser Mater Sci Eng* 1198: 012006. https://doi.org/10.1088/1757-899X/1198/1/012006
17. Chimytov TA, Nomoev AV, Bazarova DZ, et al. (2023) Investigation of the dielectric properties of polymer-dispersive liquid-crystal films dopated with silicon dioxide nanoparticles. *Tech Phys* 69: 1157–1163. https://doi.org/10.1134/S106378422404008X
18. Israelachvili JN (2011) *Intermolecular and Surface Forces*, 3 Eds., Waltham, MA: Academic Press, 81–82. https://doi.org/10.1016/C2009-0-21560-1

AIMS Press